

Progress toward commissioning and plasma operation in NSTX-U

This content has been downloaded from IOPscience. Please scroll down to see the full text.

View [the table of contents for this issue](#), or go to the [journal homepage](#) for more

Download details:

IP Address: 198.125.233.17

This content was downloaded on 09/07/2015 at 19:55

Please note that [terms and conditions apply](#).

Progress toward commissioning and plasma operation in NSTX-U

M. Ono¹, J. Chrzanowski¹, L. Dudek¹, S. Gerhardt¹,
P. Heitzenroeder¹, R. Kaita¹, J.E. Menard¹, E. Perry¹,
T. Stevenson¹, R. Strykowski¹, P. Titus¹, A. von Halle¹,
M. Williams¹, N.D. Atnafu¹, W. Blanchard¹, M. Cropper¹,
A. Diallo¹, D.A. Gates¹, R. Ellis¹, K. Erickson¹, J. Hosea¹,
R. Hatcher¹, S.Z. Jurczynski¹, S. Kaye¹, G. Labik¹, J. Lawson¹,
B. LeBlanc¹, R. Maingi¹, C. Neumeyer¹, R. Raman²,
S. Raftopoulos¹, R. Ramakrishnan¹, A.L. Roquemore¹,
S.A. Sabbagh³, P. Sichta¹, H. Schneider¹, M. Smith¹,
B. Stratton¹, V. Soukhanovskii⁴, G. Taylor¹, K. Tresemer¹,
A. Zolfaghari¹ and The NSTX-U Team

¹ Princeton Plasma Physics Laboratory, PO Box 451, Princeton, NJ 08543, USA

² University of Washington at Seattle, Seattle, WA 98195, USA

³ Columbia University, New York, NY 10027, USA

⁴ Lawrence Livermore National Laboratory, Livermore, CA 94551, USA

E-mail: mono@pppl.gov

Received 17 December 2014, revised 22 April 2015

Accepted for publication 4 May 2015

Published 5 June 2015



CrossMark

Abstract

The National Spherical Torus Experiment-Upgrade (NSTX-U) is the most powerful spherical torus facility at PPPL, Princeton USA. The major mission of NSTX-U is to develop the physics basis for an ST-based Fusion Nuclear Science Facility (FNSF). The ST-based FNSF has the promise of achieving the high neutron fluence needed for reactor component testing with relatively modest tritium consumption. At the same time, the unique operating regimes of NSTX-U can contribute to several important issues in the physics of burning plasmas to optimize the performance of ITER. NSTX-U further aims to determine the attractiveness of the compact ST for addressing key research needs on the path toward a fusion demonstration power plant (DEMO). The upgrade will nearly double the toroidal magnetic field B_T to 1 T at a major radius of $R_0 = 0.93$ m, plasma current I_p to 2 MA and neutral beam injection (NBI) heating power to 14 MW. The anticipated plasma performance enhancement is a quadrupling of the plasma stored energy and near doubling of the plasma confinement time, which would result in a 5–10 fold increase in the fusion performance parameter $n\tau T$. A much more tangential 2nd NBI system, with 2–3 times higher current drive efficiency compared to the 1st NBI system, is installed to attain the 100% non-inductive operation needed for a compact FNSF design. With higher fields and heating powers, the NSTX-U plasma collisionality will be reduced by a factor of 3–6 to help explore the favourable trend in transport towards the low collisionality FNSF regime. The NSTX-U first plasma is planned for the Summer of 2015, at which time the transition to plasma operations will occur.

Keywords: NSTX-U, spherical tokamak, FNSF

(Some figures may appear in colour only in the online journal)

1. Introduction

After over a decade of operations, the NSTX facility has undergone significant upgrades. The National Spherical Torus Experiment facility [1, 2] has entered its final construction phase, and preparation for plasma operations is now underway. The NSTX facility [3], which operated since 1999, has concluded its operation in 2011. The major mission of NSTX-

U is to develop the physics basis for an ST-based Fusion Nuclear Science Facility (FNSF) [4, 5]. The ST-based FNSF has the promise of achieving the high neutron fluence needed for reactor component testing with relatively modest tritium consumption. At the same time, the unique operating regimes of NSTX-U can contribute to several important issues in the physics of burning plasmas to optimize the performance of ITER. The NSTX-U program also aims to determine the

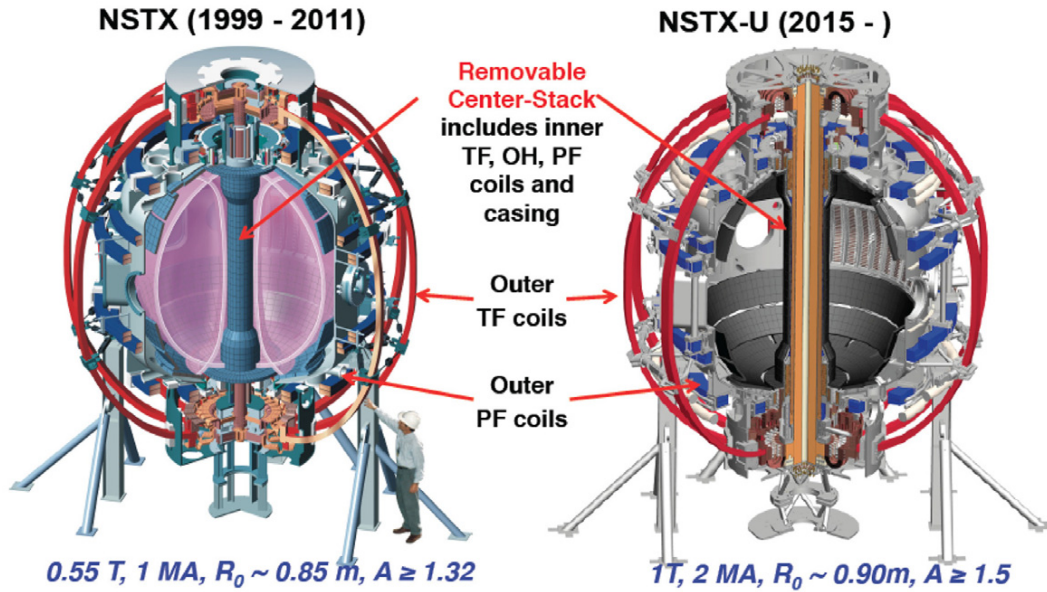


Figure 1. Schematics of NSTX and NSTX-U devices.

attractiveness of the compact ST for addressing key research needs on the path toward a fusion demonstration power plant (DEMO).

2. Overview of NSTX-U facility capability

Schematics of the NSTX and NSTX-U facilities are shown in figure 1, and their respective device and plasma parameters are shown in table 1. The main changes are the replacement of the centre-stack and the addition of the 2nd neutral beam injection (NBI) system. The new centre-stack with a four times larger TF coil cross section (as shown in figure 2) and three times larger ohmic flux, permits the doubling of the TF from ~ 0.5 to 1 T and the plasma current I_p from 1 to 2 MA, while expanding the plasma pulse length from ~ 1 to 5 s. As can be seen in the figure, NSTX-U retains the basic configuration of NSTX, as much of the NSTX facility is utilized including the vacuum vessel (VV) and outer TF and PF coils. The outer TF legs and PF coils were originally designed to support the increased current levels. However, the VV and associated magnetic field (outer TF and PF) coil support structures were enhanced in order to handle the anticipated four times greater electromagnetic forces compared to NSTX. The addition of a 2nd NBI system (figure 3) will not only double the NBI heating power from 7 to 14 MW, but the strong tangential injection will increase the current drive efficiency by ~ 1.5 –2 to enable non-inductive operation. The anticipated plasma performance enhancement is a quadrupling of the plasma stored energy and near doubling of the plasma confinement time, which would result in a 5–10 fold increase in the well-known fusion performance parameter $n\tau T$. Even though the size of NSTX-U remains relatively compact, with ~ 1 T toroidal magnetic fields and $\sim 25\%$ toroidal beta values, the absolute plasma pressure expected in NSTX-U could be comparable to that of the present day tokamaks. This would assure that the exciting

contributions of NSTX-U will continue to be at the forefront of the world fusion program.

3. Four major physics goals of NSTX-U

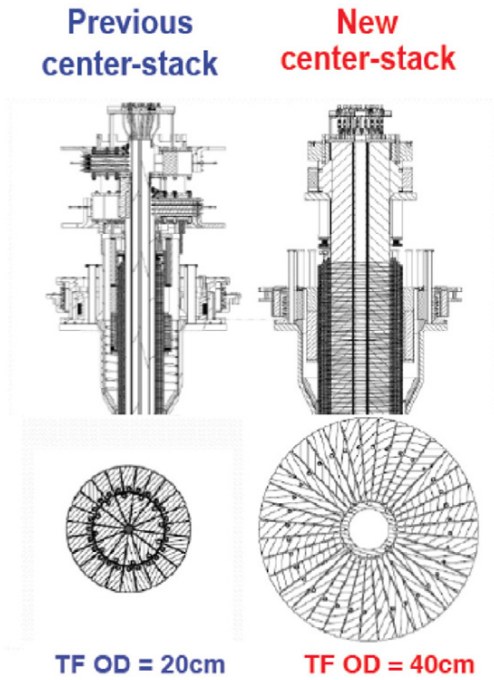
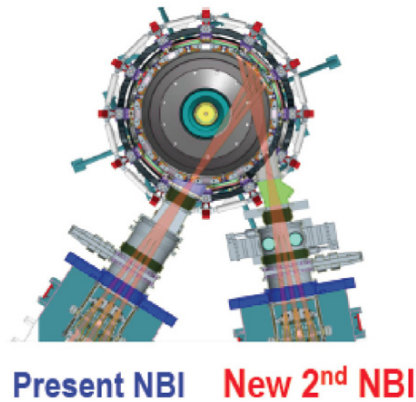
The NSTX-U facility is designed to address four major physics goals/issues for tokamak/ST-based FNSF and fusion reactor systems [1, 2]:

3.1. Demonstration of stability and control for steady-state high β plasmas

With the addition of the strongly tangential 2nd NBI beam system, NSTX-U is designed to attain 100% non-inductive operation at reactor-relevant high β plasmas. To achieve high bootstrap current fraction discharges, it is necessary to access high β_N and high κ , i.e. $f_{BS} \propto A^{-0.5}(1 + \kappa^2)\beta_N^2/\beta_T$ where κ is the plasma elongation and β_N is a normalized beta. In figure 4, previously achieved κ and β_N values in NSTX are shown as triangles and squares, and operating points of various FNSF and pilot plant design studies are shown as diamonds [6]. The expected operating spaces of NSTX-U are shown as dotted squares. As can be seen from the figure, NSTX has achieved the $\kappa \sim 2.8$ and $\beta_N \sim 5$ needed for those facilities. The previous NSTX experiments have demonstrated $\sim 50\%$ bootstrap current fraction (f_{BS}) as required for FNSF and the non-inductive current fraction f_{NI} of up to 70%. NSTX-U will aim to extend κ to ~ 3.0 and β_N to ~ 6 in the $A \sim 1.7$ range at higher plasma current and magnetic field. With the expected electron energy confinement improvement due to the doubling of toroidal magnetic field, together with the factor of ~ 2 improved current drive efficiency of the second NBI system, 100% non-inductive operation should be attainable at ~ 1 MA plasma current in NSTX-U [2]. NSTX-U is also equipped with a set of six non-axisymmetric (3D) control coils, which can be independently powered to actively control resistive wall

Table 1. NSTX and NSTX U parameters.

	R_0 (m)	A_{\min}	I_p (MA)	B_T (T)	t_{TF} (s)	R_{cs} (m)	R_{OB} (m)	OH flux (Wb)
NSTX	0.854	1.32	1	0.55	1	0.185	1.574	0.75
NSTX-U	0.934	1.5	2	1	6.5	0.315	1.574	2.1

**Figure 2.** Schematics of NSTX and NSTX-U centre-stack with inner TF coil cross section views.**Figure 3.** Schematics of present and 2nd NBI systems on NSTX-U.

modes (RWMs) at high beta [7], control error fields [8], and apply resonant magnetic perturbations for plasma rotation [9] and edge localized mode (ELM) control [10].

3.2. Plasma energy confinement physics at low plasma collisionality, especially electron energy transport

In NSTX and MAST, the electron energy confinement has improved with reduced collisionality in H-mode plasmas [11, 12]. Importantly, the lithium plasma facing component

(PFC) coating also significantly improved electron energy confinement for H-mode plasmas in NSTX by $\sim 30\%$ [13]. This electron energy confinement improvement with lithium appears to be consistent with the favourable collisionality scaling [14]. Also in NSTX, the enhanced pedestal H-mode was observed to have an increase in the H-mode confinement factor H by $\sim 50\%$ [15]. With higher fields and heating powers, the NSTX-U plasma collisionality will be reduced by a factor of 3–6 to help explore the favourable trend in transport towards the low collisionality FNSF regime. The understanding of electron transport physics is especially critical for predominantly electron heated reactor plasmas, including ITER. If the favourable trends observed on NSTX hold at low collisionality, good plasma confinement could be achieved in very compact ST devices as shown in figure 5 [1]. The ITER confinement scaling curve is for indication only since its scaling is with average, not electron, collisionality.

3.3. Divertor solutions for mitigating high heat flux

The total auxiliary heating power of 20 MW provided by the NBI and high-harmonic fast wave (HHFW) systems will allow NSTX-U to uniquely produce reactor-relevant high divertor heat fluxes of $\sim 40 \text{ MW m}^{-2}$. With the expected steady-state divertor heat flux limit for solid and liquid divertor PFCs to be $\leq 10 \text{ MW m}^{-2}$, it is essential to investigate innovative divertor heat mitigation concepts in NSTX-U. Those divertor heat flux limits could be further influenced by the high neutron environment expected in reactors. In NSTX, a snow-flake divertor configuration which provides a divertor flux expansion f of up to ~ 50 was investigated, demonstrating a significant divertor heat flux reduction of $\sim \times 3$ as shown in figure 6 [16]. It should be noted that the base value of flux expansion is ~ 10 –15 for NSTX due to the ST geometry. This is consistent with the inversely proportional to f peak heat flux reduction [17]. In NSTX-U, the snow-flake configuration will be tested with an up-down symmetric configuration which, with adequate control, should provide another factor of 2 heat flux reduction. NSTX-U will also continue to explore the use of lithium PFC coating techniques for enhanced plasma performance, and divertor power and particle handling [18, 19]. A lithium granular injector will be implemented for ELM pacing at high injection rate to control impurities and reduce the peak ELM heat flux.

3.4. Non-inductive start-up, ramp-up, and sustainment

With relatively small or no central OH solenoid capability expected in a compact lower aspect-ratio ($A \equiv R_0/a$) tokamak and/or ST reactors, it is crucial to demonstrate plasma start-up without use of a central solenoid. As shown in figure 7, the solenoid-free start-up, ramp-up, and sustainment scenario for NSTX-U employs a number of tools including CHI, ECH, HHFW, and NBI as will be described in section 5. In NSTX,

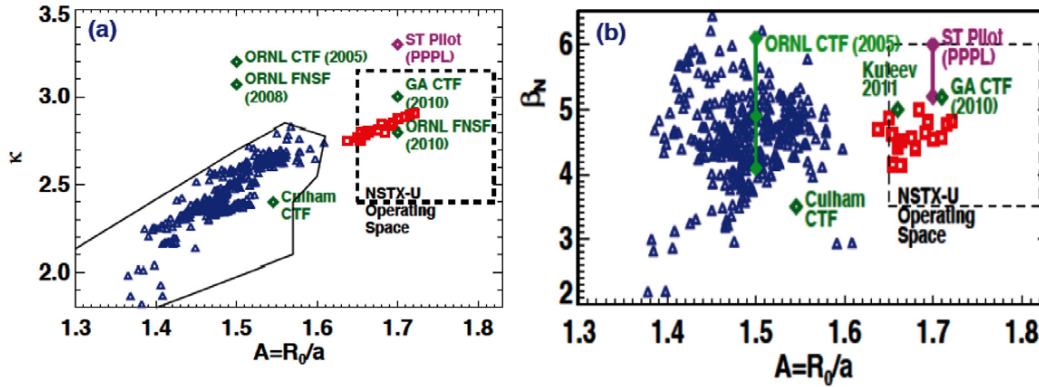


Figure 4. Bootstrap current relevant parameters $\kappa \sim 3$ and β_N achieved in NSTX. The FNSF and power plant operating parameters are as labelled. The expected NSTX-U operational spaces are indicated by the dotted squares. Reprinted with permission from [6]. Copyright 2011 Institute of Physics.

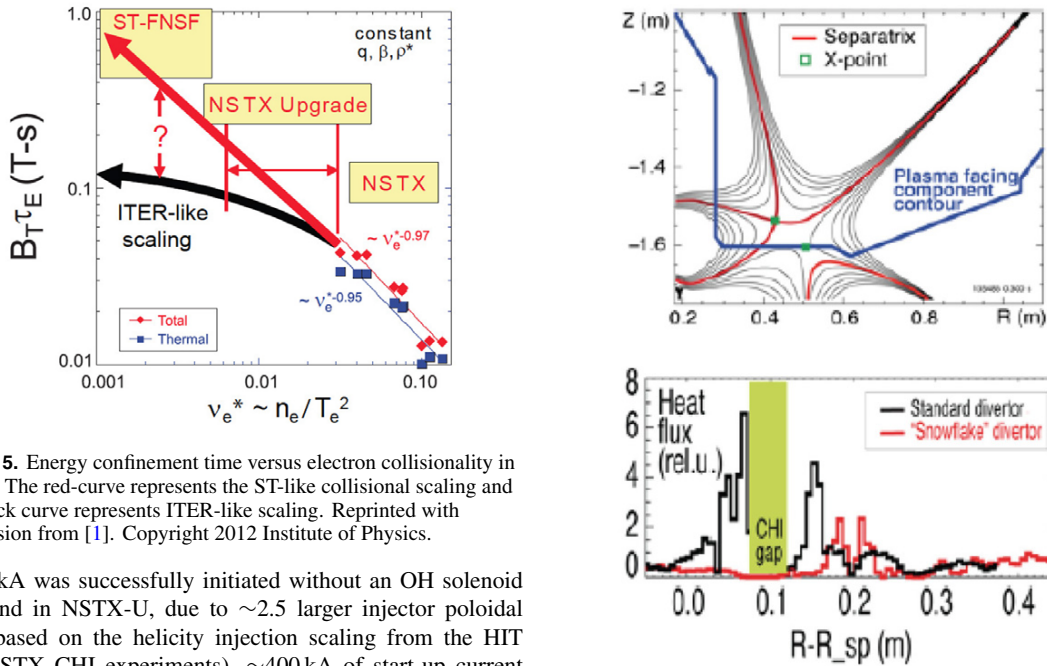


Figure 5. Energy confinement time versus electron collisionality in NSTX. The red-curve represents the ST-like collisional scaling and the black curve represents ITER-like scaling. Reprinted with permission from [1]. Copyright 2012 Institute of Physics.

~ 160 kA was successfully initiated without an OH solenoid [20] and in NSTX-U, due to ~ 2.5 larger injector poloidal flux (based on the helicity injection scaling from the HIT and NSTX CHI experiments), ~ 400 kA of start-up current is anticipated [21]. With ~ 1 MW level ECH heating, the CHI plasma is projected to be heated to a few hundred eV. Target plasmas thus formed will be further heated with HHFW to the keV range and NBI will be then applied for further current ramp-up and eventual sustainment of \sim MA level plasma current at high beta, with ~ 70 – 80% bootstrap current fractions. The same scaling suggests ~ 1 – 2 MA of start-up current should be achievable in FNSF with CHI. At this current level, the main (~ 0.5 MeV) NBI heating and current drive can commence for current ramp-up and steady-state operation. It should be noted that another helicity injection concept termed local helicity injection (LHI) is being developed on PEGASUS [22]. It successfully created a plasma current of ~ 160 kA in PEGASUS, and a gun for NSTX-U is under development to achieve 0.5 – 1.0 MA of start-up plasma current. If successful, helicity injection can not only enable an ST-based FNSF, but also may simplify the design of conventional aspect ratio tokamak reactors.

Figure 6. Snow-flake divertor configuration (above) and measured divertor flux comparison with standard configuration. Reprinted with permission from [33]. Copyright 2011 Institute of Physics.

4. NSTX-U Upgrade Construction Project

4.1. New centre-stack fabrication

A schematic of the new centre-stack is shown in figure 8. It is composed of an inner TF coil bundle, an OH solenoid, up-and-down symmetric PF 1a, 1b, and 1c coils, and a CS casing [23]. The upper and lower PF 1a, 1b, and 1c coils enable finer divertor control, including the double snow-flake configuration, as well as improved CHI performance.

4.1.1. TF bundle fabrication. The inner TF bundle utilizes 36 wedge-shaped OFHC copper and the lead extension stubs from a higher strength copper alloy (Cu–Cr–Zr). Each TF

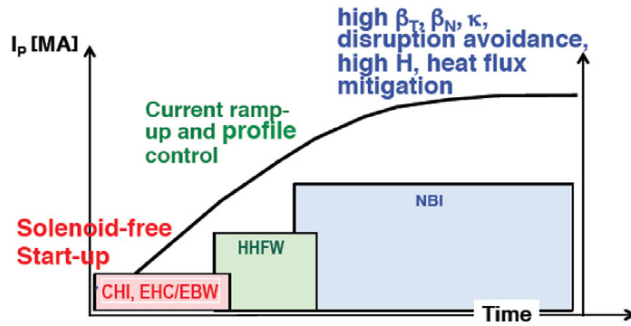


Figure 7. A scheme for the fully non-inductive operation scenario in NSTX-U.

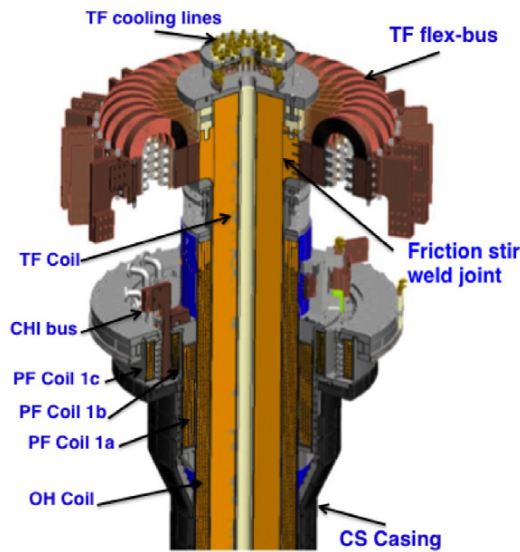


Figure 8. A schematic of the new centre-stack and the TF joint area.

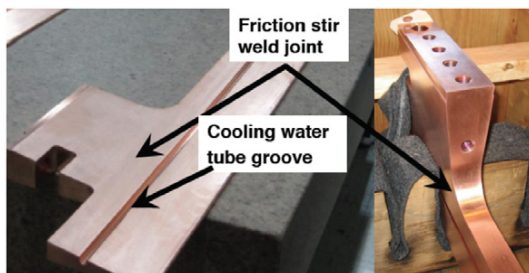


Figure 9. A TF bar with friction stir welded lead extension and cooling tube groove.

conductor requires a welded connection to a lead extension stub on both ends. A metal joining technique called friction stir welding (which avoids annealing) was employed. In figure 9, a completed TF conductor bar is shown. A cooling passage with a copper tube was soldered into a length-wise groove on one side of the TF conductor wedge, with a specially developed eutectic (96Sn/4Ag) solder paste formulated with non-ionic flux [24]. This utilization of non-ionic flux was motivated by the previous electrical insulation failure in the NSTX TF bundle, where the residual Zn-Cl based flux caused

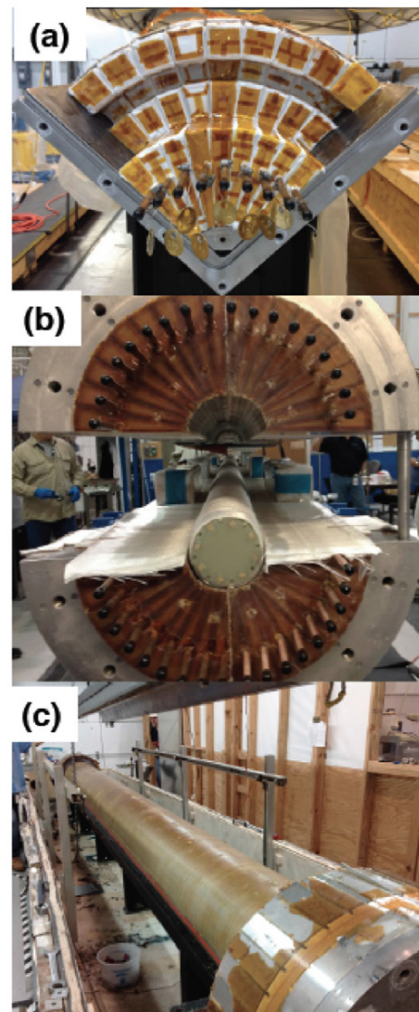


Figure 10. TF fabrication stages (a) insulated TF quadrant prior to VPI (b) assembly of full bundle, (c) TF bundle after VPI.

gradual deterioration of the insulation material over ~ 7 years of operations. The assembly of the centre-stack was carried out at a specially prepared coil shop with a clean preparation room and an oven room at PPPL. A TF quadrant section was assembled with nine conductors placed into a quadrant mold as shown in figure 10(a). The quadrant construction was chosen to maintain the high tolerance required for the TF bundle. Each TF quadrant was successfully vacuum pressure impregnated (VPI) with CTD 425, which is a 3 cyanate ester-epoxy blend with long service life and low viscosity to aid the impregnation process. The four completed quadrants were then assembled together to complete the full TF bundle as shown in figure 10(b). The full TF bundle after VPI is shown in figure 10(c). After completing the TF bundle in 2013, the winding of the OH coil over the full TF bundle was performed in 2014.

4.1.2. OH-coil winding. The upgraded OH coil is designed for 6077 V @ 24 000 A, providing poloidal flux of ~ 2.1 V-s which is $\sim 3\times$ that of NSTX. The start of the OH coil winding

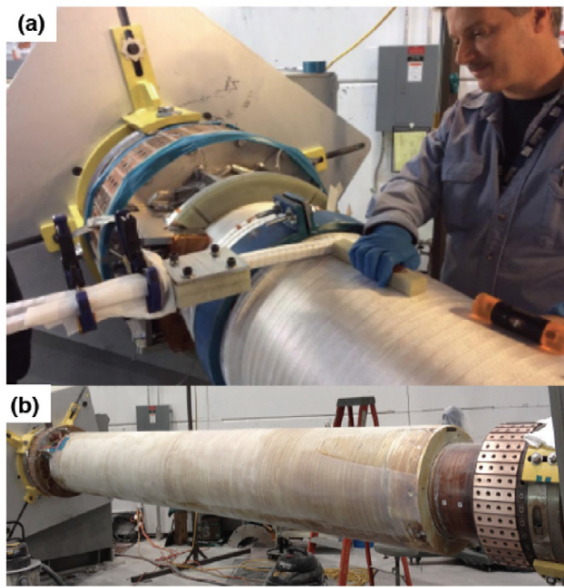


Figure 11. OH Winding (a) start of the two-in-hand OH winding. (b) Completed OH coil after VPI.

is shown in figure 11(a). The Aquapour mandrel material is designed to easily wash away after coil curing to leave an air gap between the TF bundle and OH coil for thermal expansion and motion between the two coils. Once the Aquapour has been removed, the TF bundle is supported externally at the top and bottom of the centre-stack to centre it within the OH coil. After the OH winding was completed, a VPI of the entire TF-OH centre-bundle was successfully conducted as shown in figure 11(b). It should be noted that after VPI, it was found that the epoxy penetrated the Aquapour. This made the Aquapour removal by simply dissolving with water no longer possible. The impact of leaving the Aquapour in place on the NSTX-U operations was evaluated. The axial tension stress in the OH, generated due to the thermal growth of coils must be controlled by keeping the OH coil temperature at or above that of the TF. Based on the analyses of the NSTX-U plasma scenarios and subsequent insulation stress and temperature tests, it was concluded with a high degree of confidence that all of the NSTX-U physics objectives and full operations can be met with the Aquapour in place. The presence of the Aquapour has some advantages in providing robust centering support for the OH with respect to the TF. The decision therefore was made to leave the material in place. The TF and OH coils were electrically tested successfully to full test voltages of 4.5 kV and 13 kV, respectively. This test voltage was decided utilizing the industry motivated $2\times$ operating voltage +1 kV rule. The TF test voltage was higher considering the 1 kV operating voltage to accommodate coaxial helicity injection experiments.

4.1.3. TF flex joints. To complete the TF coil, the inner TF bundle is connected to the outer TF legs using 32 upper and 32 lower high strength Cu–Zr copper alloy flex joints as shown in figures 8 and 13. The flex joint has to accommodate the vertical cyclic movement due to the growth of the TF

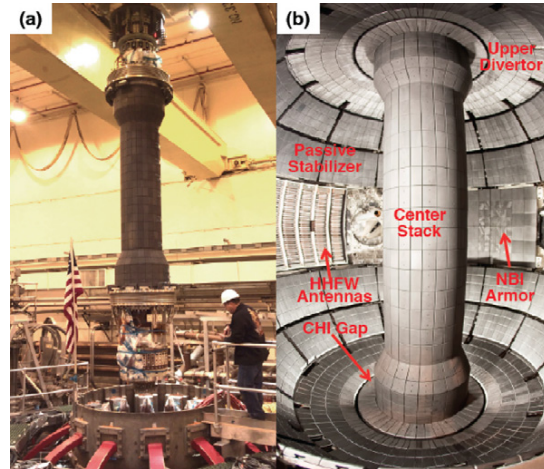


Figure 12. (a) NSTX-U centre-stack lowering into the vacuum vessel. (b) NSTX-U centre-stack installed.

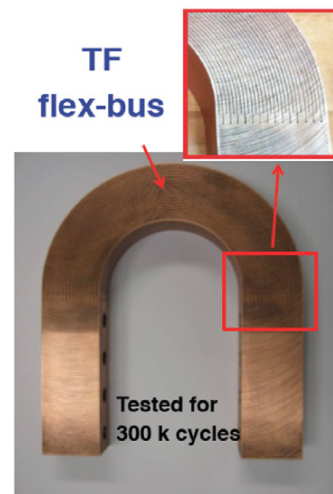


Figure 13. NSTX-U TF flex bus with EDM cuts.

bundle (~ 1.7 cm) during the operation, while resisting the $j \times B$ force of ~ 141 kA of current through the joint. The TF flex connection was fabricated from a solid U-shaped copper alloy piece by making 16 precision parallel cuts via electric discharge machining (EDM). The flex joint has successfully passed a $\sim 300\,000$ cycle fatigue test.

4.1.4. NSTX-U device structural enhancements. In order to handle the anticipated $4\times$ greater electromagnetic forces for NSTX-U compared to NSTX, the VV and associated magnetic field coil support structures were enhanced accordingly. The umbrella structure reinforcements, and PF 2/3 support upgrade hardware and PF 4/5 support upgrade hardware enhancements were implemented. Two new outer TF legs were fabricated and installed to replace the ones with cooling water leak and electrical insulation issues. The outer TF leg support upgrades were also fabricated and installed. The TF-VV clevises to better support outer TF legs were welded onto the vessel. The new, much more robust umbrella legs were installed on the machine. The VV leg attachment connections were modified

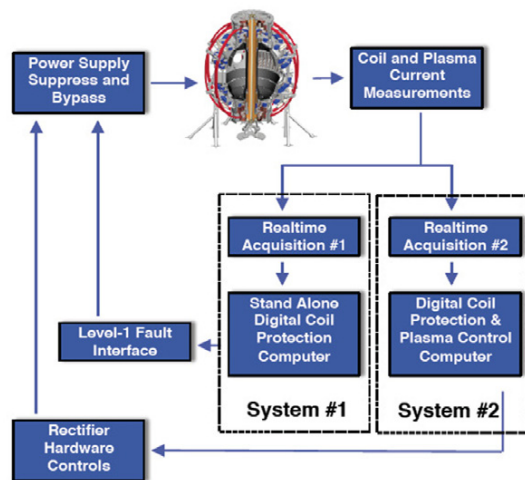


Figure 14. Schematic of the NSTX-U digital coil protection system providing comprehensive coil protection against electromagnetic loads and thermal limits.

to clear the clevises. In addition, since the plasma disruption forces are also expected to increase by a factor of 4, the internal passive plates were reinforced by replacing the stainless steel attachment hardware with Inconel versions using appropriate model extrapolation from the measure NSTX values.

4.1.5. Digital coil protection system. As the device size and plasma performance capability increase, the device protection becomes highly complex and challenging. With four times the magnetic forces and energy, and the expected disruption loads, NSTX-U device protection is no longer possible with the individual power supply limit control approach used in NSTX. The disruption loads were estimated based on the actual measured NSTX values, appropriately scaled to the NSTX-U conditions in terms of β_T , I_p , and A . This was feasible because the basic vacuum chamber and passive plate configurations were unchanged from NSTX. To protect NSTX-U from unintended operational conditions due to the power supplies delivering current combinations that create forces or stresses beyond the design-basis, a digital coil protection system (DCPS) is implemented [25]. The DCPS is designed to prevent accidental (either human or equipment failure) overload beyond the design conditions of the structure which currents from the power supply system could generate, even while each individual power supply is operating within its allowable current range as shown in figure 14. Initially, the DCPS algorithms will test approximately 125 force and stress calculations against limit values, using both two models for the plasma shape and two models for potential post-disruption currents; this results in 500 total force/stress calculations in addition to 14 thermal limit calculations. The update rate of each type will be $200 \mu\text{s}$ for both the force-based and the thermal-based signals. Redundant current measurements for each coil and plasma current will be provided as inputs. This type of sophisticated real time coil protection system, if fully demonstrated, could be utilized for safe operation of future fusion devices including ITER.



Figure 15. In-vessel view of the tangential injection port of the 2nd NBI.

4.1.6. Power system upgrades. The NSTX-U power systems include 68 identical rectifiers (Transrex ac/dc Converters), providing a total pulsed power capability of 1650 MVA for 6 s every 300 s. New firing generators (FGs) were installed for the precise control of thyristor firing angles needed for NSTX-U operations that are particularly critical for the 8-parallel, 130 kA TF system configuration. The new FG delivers firing pulses with far greater resolution, precision, and repeatability than the previous ones in NSTX. In addition, a TF turn-to-turn fault detection and trip has been designed and installed. The NSTX-U 475 MVA/pulse motor generator with weld cracks was also repaired. The motor generator repair brought the motor generator set to its original specifications to enable full field operation for NSTX-U.

4.2. Neutral beam injection system upgrade

The 2nd NBI upgrade scope is to add a complete, functional second beam-line (BL), which was previously used in the TFTR DT-campaign, to NSTX-U at aiming tangency radii of 110, 120, and 130 cm compared to 50, 60, and 70 cm for the present 1st NBI. A schematic of the present and new 2nd NBI systems are shown in figure 3. This task largely utilizes the existing TFTR NBI infrastructure. To accommodate the strongly tangential injection, a specially designed ‘bay-window’ was installed as shown in figure 15 [26]. By moving the VV wall out by ~ 12 cm, a potential issue of the clipping of the outer most beam by the VV was avoided. The redesigned and relocated NBI armor for shine-through protection, to capture both sets of NBI heat deposition profiles while maintaining the same level of VV wall protection, is shown in figure 12(b) [27]. The 2nd NBI tasks included the TFTR NBI BL tritium decontamination, refurbishments, sources, relocation, services, power and controls, and NSTX-U Test Cell (NTC) rearrangements. In addition, there are VV modifications, the NBI and torus vacuum pumping system ducts, and NBI armour. The 2nd NBI BL (BL2) refurbishment and relocation have been completed.

The recent NSTX-U test cell aerial view is shown in figure 16 where the 2nd NBI installation and device construction are complete.

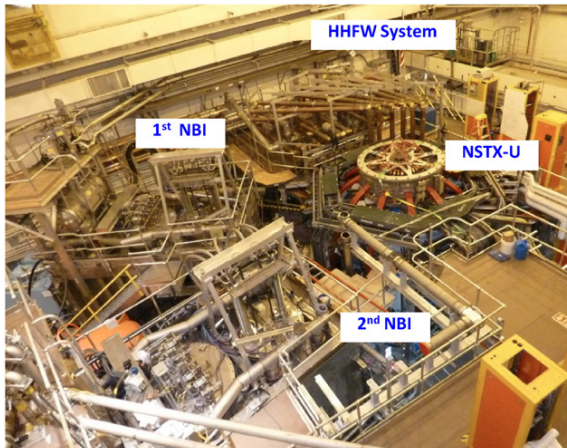


Figure 16. Aerial view of the NSTX-U Test Cell, March 2015.

5. Additional science facility enhancements

In addition to the facility upgrades described above, there are other important research facility capabilities required to address the NSTX-U mission elements. Perhaps the most challenging and potentially most important one is solenoid-free high beta operations as required for the ST-based FNSF and power plants. This area of research also could benefit advanced tokamak scenario development. Solenoid-free start-up is critical for the ST-based compact FNSF, since there is no room for the central solenoid and associated neutron shielding as described in section 5.1. The current ramp-up to an intermediate current level with HHHW is highly important to bridge the gap between the start-up plasma and the minimum current level (~ 400 kA for NSTX-U and 1–2 MA for an ST-FNSF) required to turn on the main NBI beams for heating and current drive as described in section 5.2. In section 5.3, the resistive wall mode (RWM) stabilizing coils are described; they are used to achieve high beta plasmas needed for high f_{BS} discharges without disruptions. In section 5.4, we describe the divertor heat flux mitigation tools. Finally, we will summarize the diagnostics being readied for NSTX-U in section 5.5.

5.1. Solenoid-free start-up with CHI

For non-inductive start-up, the coaxial helicity injector (CHI) is prepared to support plasma start-up currents well over the 400 kA required to couple a CHI started discharge to non-inductive current ramp-up [20]. This projection is based on the helicity injection balance model thus far confirmed in the HIT and NSTX CHI experiments. The baseline PFCs for the initial NSTX-U operation are graphite tiles. Because of the increased plasma heat loads due to the increased NBI heating power and pulse duration, it was decided to enhance the protection of the ‘CHI Gap’. The CHI Gap is the region between the NSTX-U inner and outer VVs, above or below the CHI insulators as shown in figures 12(b) and 17(a). The graphite tiles on both the inner and outer divertors are extended downwards, coming in close contact to the PF-1C coil casing and stainless steel outer vessel flanges and shielding these components from plasma contact. This narrower and deeper CHI gap will protect the

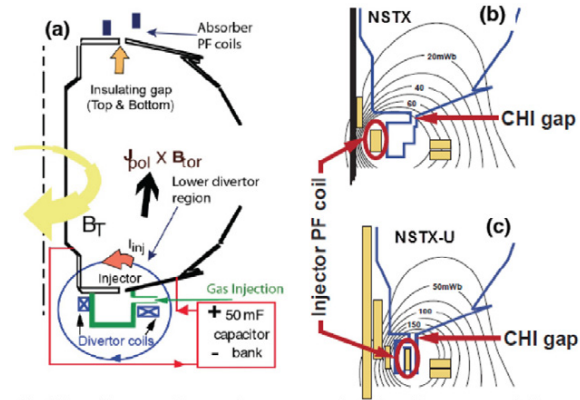


Figure 17. NSTX-U CHI schematics. (a) A schematic of CHI set-up where the centre-stack is electrically biased against outer vacuum vessel. The electrical discharge established is expelled into the main chamber by the $j_{pol} \times B_T$ force. (b) and (c) A comparison of poloidal flux pattern between NSTX and NSTX-U.

vessel and PF-1C coil from excessive heat flux and protect the plasma from metal contamination, while continuing to provide the capability for CHI operations. A comparison of the poloidal injector flux contours are shown for NSTX and NSTX-U in figure 17(b) and (c). The injector flux is about 2.5 times larger for NSTX-U compared to that of NSTX. The enhanced injector flux should result in proportionately larger helicity injection and, therefore, the achievable start-up current. Due to the anticipated higher CHI start-up current and required bias-voltage (~ 3 kV in NSTX-U compared to ~ 2 kV in NSTX), the centre-stack magnet insulation is enhanced accordingly.

5.2. HHHW and ECH for current ramp-up

A 6 MW HHHWs system is being prepared for electron heating and current ramp-up [28]. While the HHHW system is basically unchanged, the antenna feed-thru conductors were modified to be able to handle the higher disruption loads ($\sim \times 4$) in NSTX-U. To handle those disruption loads, compliant connectors were designed, tested, and installed between the feed-throughs and antenna straps for the NSTX-U operation. In order to increase the power from the existing 12-strap HHHW antenna, the rf voltage stand-off was tested on an rf test stand with the new compliant feeds. The test demonstrated rf voltage stand-off of 46 kV, which is about twice the value required. The HHHW antenna system with the compliant feeds and improved back plate grounding were installed in NSTX-U, as shown in figures 12(b) and 18. The tests also showed rf-induced arc-prone areas behind the back-plate. For improved rf diagnostics, rf probes and tile sensors were also installed. In NSTX, while HHHW was able to heat the ohmic 200–300 eV plasmas, it was not able to directly heat the relatively cold ~ 30 –50 eV CHI plasmas. This is consistent with the theoretical expectations for HHHW heating. To bridge the temperature gap, electron cyclotron heating (ECH) at ~ 1 MW level will be implemented to heat the CHI-created plasma to 200–300 eV range so that the HHHW for electron heating and current ramp-up can couple into the CHI start-up plasmas.

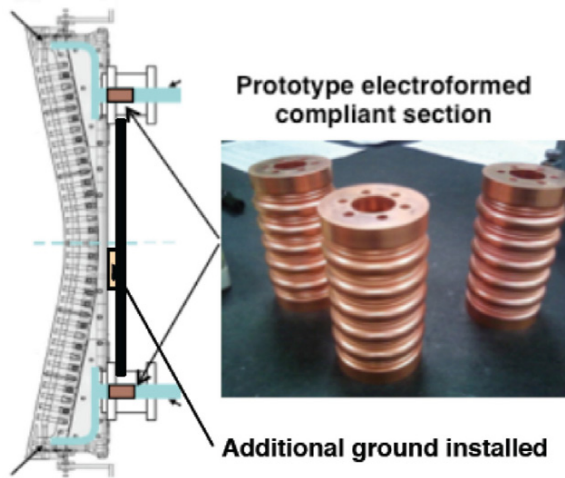


Figure 18. A schematic of HHFW antenna with improved antenna feeds (photograph) and backplate ground.

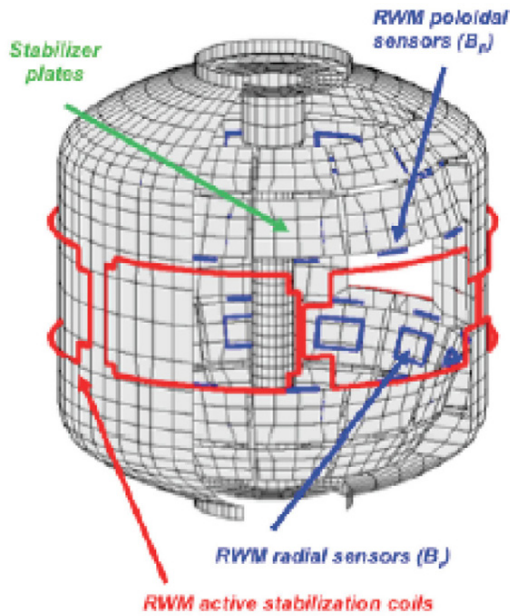


Figure 19. Diagram of NSTX showing internal B_r and B_θ sensors, passive stabilizing plates and ex-vessel 3D control coils.

5.3. Tools for high-beta/high bootstrap current fraction operations

To support high beta NSTX-U operation, a number of macro-stability control tools are being prepared. Mid-plane RWM control coils (shown in figure 19) and resulting equilibria require re-computation of $n = 1$ active RWM control performance using proportional gain, and RWM state space control [7]. The upgrade also adds new capabilities, such as independent control of the 6 RWM coils with six switching power amplifier (SPA) sources. These new capabilities, combined with the upgrade of the RWM state space controller, will also allow simultaneous $n = 1$ and $n = 2$ active control, along with $n = 1, 2,$ and 3 dynamic error field correction.

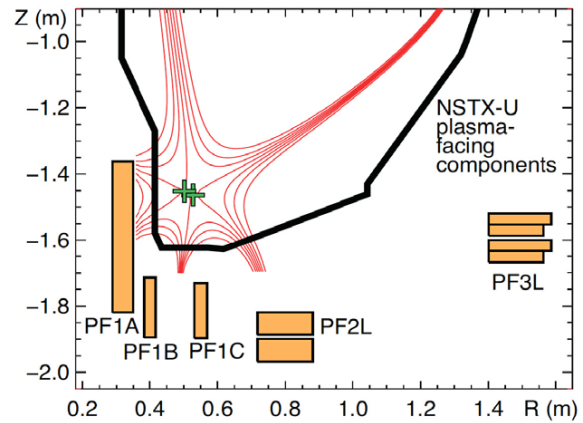


Figure 20. Snow-flake divertor configuration in NSTX-U.

Finally, the active control performance of the proposed off-mid-plane non-axisymmetric control coils (NCC) also needs to be evaluated. A significant increase in controllable β_N is expected with the RWM state space control in NSTX-U, as was found for NSTX.

5.3.1. Disruption mitigation systems. A key issue for ITER, and the tokamak/ST line of fusion devices in general, is the avoidance and mitigation of disruptions. Most of the disruptions are expected to be mitigated by massive gas injection (MGI) [29]. In support of the planned MGI Experiments on NSTX-U, the University of Washington has successfully built and tested an electromagnetic MGI valve for installation on NSTX-U. The NSTX-U MGI systems employ for the first time a ‘double-solenoid’ design developed by ORNL for the ITER MGI system [30]. This double solenoid design cancels the $j \times B$ force on the MGI body and therefore should be suitable for operations in high magnetic fields (e.g. for ITER). Another unique feature of the NSTX-U MGI system is the ability to investigate the poloidal dependence of the effectiveness of MGI in tokamaks. To measure disruption characteristics in detail, an extensive array of disruption diagnostics including halo current sensors and magnetic probe arrays have been installed. In addition to the outer mid-plane, a MGI with the same injector configuration was installed in the lower divertor region. The lower MGI can be also used to investigate the effectiveness of higher field inboard injection as well as in the private region injection. In addition, a much higher conductance MGI was installed at the upper divertor region to investigate the merit of faster MGI. The valves were installed on NSTX-U after undergoing off-line tests at the Univ. of Washington.

5.4. Novel power exhaust solutions

In NSTX-U, the projected peak divertor heat fluxes can reach $20\text{--}40 \text{ MW m}^{-2}$ with $I_p \leq 2 \text{ MA}$, and $P_{\text{NBI}} \leq 12 \text{ MW}$, with pulse length up to 5 s. NSTX-U will explore novel solutions to the boundary physics power exhaust challenge by testing the so-called ‘snowflake’ (SF) divertor configuration, and liquid metal PFCs to mitigate erosion and melting problems.

Table 2. NSTX-U diagnostics.

MHD/Magnetics/Reconstruction	Edge Divertor Physics
Magnetics for equilibrium reconstruction	Gas-puff imaging (500 kHz)
Halo current detectors	Langmuir probe array
High- n and high-frequency Mirnov arrays	Edge rotation diagnostics (T_i , V_ϕ , V_{pol})
Locked-mode detectors	1D CCD H_α cameras (divertor, midplane)
RWM sensors	2-D divertor fast visible camera
Profile diagnostics	Metal foil divertor bolometer
MPTS (42 ch, 60 Hz)	AXUV-based Divertor Bolometer
T-CHERS: $T_i(R)$, $V_\phi(r)$, $n_C(R)$, $n_{Li}(R)$, (51 ch)	IR cameras (30 Hz) (3)
P-CHERS: $V_\theta(r)$ (71 ch)	Fast IR camera (two colour)
MSE-CIF (18 ch)	Tile temperature thermocouple array
MSE-LIF (20 ch)	Divertor fast eroding thermocouple
ME-SXR (40 ch)	Dust detector
Midplane tangential bolometer array (16 ch)	Edge deposition monitors
Turbulence/modes diagnostics	Scrape-off layer reflectometer
Poloidal FIR high- k scattering (in 2016)	Edge neutral pressure gauges
Beam emission spectroscopy (48 ch)	Material analysis and particle probe
Microwave reflectometer,	Divertor VUV spectrometer
Microwave interferometer	Plasma monitoring
Ultra-soft x-ray arrays—multi-colour	FIRETIP interferometer
Energetic particle diagnostics	Fast visible cameras
Fast Ion D_α profile measurement (perp + tang)	Visible Bremsstrahlung radiometer
Solid-state neutral particle analyser	Visible and UV survey spectrometers
Fast lost-ion probe (energy/pitch angle resolving)	VUV transmission grating spectrometer
Neutron measurements	Visible filterscopes (hydrogen and impurity lines)
Charged fusion product	Wall coupon analysis

Table 3. NSTX-U device ramp-up plan.

	NSTX (Max)	FY2015 NSTX-U operations	FY2016 NSTX-U operations	FY2017 NSTX-U operations	Ultimate goal
I_p (MA)	1.2	~1.6	2.0	2.0	2.0
B_T (T)	0.55	~0.8	1.0	1.0	1.0
Allowed TF I^2t (MA ² s)	7.3	80	120	160	160

5.4.1. Snowflake divertors. In NSTX-U, two (upper and lower) sets of four divertor coils will be used to test up-down-symmetric snowflake (SF) divertors as shown in figure 20 [31]. In NSTX, a single lower SF divertor was investigated as seen in figure 6 [9]. The modelling projections for the NSTX-U SF divertor geometry are favourable, showing large reductions in divertor T_e and T_i , as well as peak divertor heat fluxes due to the geometric and radiation effects, both with 4% carbon impurity levels and neon or argon seeding.

5.4.2. Lithium application tools. With encouraging results in NSTX [17, 32], a number of lithium application tools are being prepared for NSTX-U. Two downward-oriented lithium evaporators (LITERS) will be re-installed. An electron beam heated upper aiming evaporator to cover the upper divertor region is being developed. The electron beam enables Li to be promptly evaporated for rapidly providing fresh lithium coatings. A lithium granule injector (LGI) for ELM pacing, which was successfully demonstrated on EAST, is being prepared for NSTX-U. The NSTX-U LGI system is capable of injecting horizontally directed spherical lithium granules (0.3–0.9 mm) at speeds of 50–150 m s⁻¹. It is anticipated that much higher pacing frequencies can eventually be achieved using the basic injector technology. Granule feeding rates (pacing frequencies) of 50–500 Hz have been achieved in laboratory tests.

5.5. Diagnostic systems

The NSTX-U diagnostic installations have been an active area of NSTX-U operational preparation. A list of the diagnostic systems which are expected to be available for NSTX-U within the first year of operation is in table 2, except for the poloidal far-infrared (FIR) high- k scattering system, which is expected in FY 2016. The multi-pulse Thomson scattering (MPTS) system was extensively modified for the new laser path to avoid the radially larger new centre-stack. Some of the acronyms used in table 2 are toroidal-charge exchange recombination spectroscopy (T-CHERS), poloidal-CHERS (P-CHERS), the motional Stark effect measurement based on collisionally induced fluorescence (MSE-CIF), MSE based on laser induced fluorescence (MSE-LIF), and multi-energy soft x-ray system (ME-SXR). Most of the NSTX diagnostics were re-installed with significant modifications/enhancements and many new ones were added. We note that at least half of those diagnostic systems have strong collaboration components. The in-vessel diagnostic installation and related calibration tasks have been completed.

6. NSTX-U plasma operation start-up planning

An operational plan toward full NSTX-U operational capability is being developed. A draft plan is shown in table 3, based on an assessment of physics needs for the first year of

operations. The 1st year goal is to operate NSTX-U with the electromagnetic forces ($I_p B_T$) at halfway between NSTX and NSTX-U limits and 50% of the NSTX-U design-point for the heating of the TF coil. This still allows NSTX to operate at $B_T \sim 0.8$ T, $I_p \sim 1.6$ MA, and a maximum flat-top duration of 3.5 s in the first year, which is far beyond the achieved NSTX parameters. The device will be inspected and refurbished as needed at the end of the each operating year. For the second year, the toroidal magnetic field will be increased to its full field value of 1 T. but with the heating of the TF coil kept to 75% of the design-point. This will allow 3 s discharges at full field and current. The same limits should allow the full 5 s discharges at $B_T \sim 0.8$ T and $I_p \sim 1.6$ MA. The device will be brought to full operational capability in the third year of NSTX-U operation.

7. Discussions and conclusions

The NSTX upgrade construction project has entered its last phase, and preparation for plasma operations is now underway. The major mission of NSTX-U is to develop the physics basis for a compact ST-based Fusion Nuclear Science Facility (FNSF). At the same time, the unique operating regimes of NSTX-U can contribute to several important issues in the physics of burning plasmas to optimize the performance of ITER. The NSTX-U program further aims to determine the attractiveness of the compact ST for addressing key research needs on the path toward a fusion demonstration power plant (DEMO). The new centre-stack will provide $\beta_T = 1$ T at a major radius of $R_0 = 0.93$ m compared to 0.55 T at $R_0 = 0.85$ m in NSTX, and will enable a plasma current I_p of up to 2 MA for 5 s compared to the 1 MA for 1 s in NSTX. A much more tangential 2nd NBI system, with 2–3 times higher current drive efficiency compared to the 1st NBI system, has been installed. NSTX-U is designed to attain the 100% non-inductive operation needed for a compact FNSF design. NSTX-U first plasma is planned for the summer of 2015, at which time the transition to plasma operations will occur.

Acknowledgments

This work was supported by DoE Contract No. DE-AC02-09CH11466.

References

- [1] Menard J.E. et al 2012 *Nucl. Fusion* **52** 083015
- [2] Gerhardt S.P. et al 2012 *Nucl. Fusion* **52** 083020
- [3] Ono M. et al 2000 *Nucl. Fusion* **40** 557
- [4] Peng Y.-K.M. et al 2011 *Fusion Sci. Technol.* **60** 441
- [5] Menard J.E. et al 2014 Configuration studies for an ST-based fusion nuclear science facility 25th IAEA Int. Conf. on Fusion Energy (St. Petersburg, Russia) FNS/1-1
- [6] Gerhardt S.P. et al 2011 *Nucl. Fusion* **51** 073031
- [7] Sabbagh S.A. et al 2013 *Nucl. Fusion* **53** 104007
- [8] Park J.-K. et al 2012 *Nucl. Fusion* **52** 023004
- [9] Zhu W. et al 2006 *Phys. Rev. Lett.* **96** 225002
- [10] Canik J.M. et al 2010 *Phys. Rev. Lett.* **104** 045001
- [11] Kaye S.M. et al 2007 *Nucl. Fusion* **47** 499
- [12] Valovic M. et al 2011 *Nucl. Fusion* **51** 073045
- [13] Maingi R. et al 2012 *Nucl. Fusion* **52** 083001
- [14] Kaye S.M. et al 2013 *Nucl. Fusion* **53** 063005
- [15] Maing R. et al 2010 *Phys. Rev. Lett.* **105** 135004
- [16] Soukhanovskii V.A. et al 2012 *Phys. Plasmas* **19** 082504
- [17] Gray T.K. et al 2011 *J. Nucl. Mater.* **415** S360
- [18] Gray T.K. et al 2014 *Nucl. Fusion* **54** 023001
- [19] Ono M. et al 2013 *Nucl. Fusion* **53** 113030
- [20] Raman R. et al 2006 *Phys. Rev. Lett.* **97** 175002
- [21] Raman R. et al 2014 *IEEE Trans. Plasma Sci.* **42** 2154
- [22] Battaglia D.J. et al 2009 *Phys. Rev. Lett.* **102** 225003
- [23] Dudek L. et al 2012 *Fusion Eng. Des.* **87** 1515
- [24] Jurczynski S.Z. et al 2013 Solder development and fabrication techniques for coolant tube bonding in toroidal field conductors for the National Spherical Torus Experiment Center Stack Upgrade *IEEE 25th Symp. on Fusion Engineering (SOFE)*
- [25] Erickson K.G. et al 2014 *IEEE Trans. Plasma Sci.* **42** 1811
- [26] Atnafu N.D. et al 2013 NSTX-U vacuum vessel design modification *IEEE 25th Symp. on Fusion Engineering (SOFE)*
- [27] Tresemer K. et al 2011 Neutral Beam Armor for NSTX Upgrade *Fusion Sci. Technol.* **60** 303
- [28] Ellis R. et al 2014 Upgrades to the NSTX HHFW antenna *AIP Conf. Proc. 20th Topical Conf. on Radiofrequency Power in Plasmas* vol 1580, p 350
- [29] Raman R. et al 2014 *Rev. Sci. Instrum.* **85** 11E801
- [30] Raman R. private communication
- [31] Soukhanovskii V.A. et al 2012 Snowflake divertor as plasma-material interface for future high power density fusion devices 2012 Proc. 24th Int. Conf. on Fusion Energy (San Diego, CA, 2012) EX/P5-21 www.naweb.iaea.org/naweb/physics/FEC/FEC2012/index.htm
- [32] Ono M. et al 2012 *Fusion Eng. Des.* **87** 1770
- [33] Soukhanovskii A. et al 2011 *Nucl. Fusion* **51** 012001